Developments of mTOR siRNA anchored PTX nanoparticles for the treatment of triple- negative breast cancer (TNBC)

Shalini Krishnan[1,2], Varatharajan Rajavel[1*], Shahrul Hamid[2], Vijayan Venugopal[3], Vasanth Raj Palanimuthu[4],

[1]*AIMST University, Semeling, 08100, Bedong, Kedah Darul Aman, Malaysia*
[2]*Oncological and AMP; Radiological Sciences Cluster, Advanced Medical & Dental Institute, Universiti Sains Malaysia, 13200 Penang, Malaysia*
[3]*School of pharmacy, Sri Balaji Vidyapeeth University, Pillayarkuppam, Puducherry 607402, India*
[4]*Dept. of Pharmaceutical Biotechnology, JSS College of Pharmacy, Ooty 643001, Tamilnadu, India*

*** Correspondence:**
Dr. Varatharajan Rajavel
Pharmacology Unit, Faculty of Pharmacy,
AIMST University, Semeling, 08100 Bedong,
Kedah Darul Aman, Malaysia.
Email: varadharajeen@gmail.com.

ABSTRACT

Introduction: Triple-negative breast cancer (TNBC) is categorized as an aggressive subtype of breast cancer that expresses EGFR receptors. mTOR siRNA loaded Paclitaxel (PTX) could be the possible way to treat TNBC. **Objective**: The aim of this study was to develop an efficient drug delivery system for specifically targeting the TNBC cells without affecting normal cells by formulating PTX - loaded PLGA (Poly (lactic-co- glycolic acid) nanoparticle bio-conjugate with mTOR siRNA. **Methods**: The nanoparticles were synthesized by double emulsification followed by solvent evaporation. The conjugated nanoparticles were characterized by physiochemical properties (size, shape, entrapment efficiency, and release studies) and cancer cell properties (Cytotoxicity, serum stability, siRNA binding efficiency). **Results and Discussion**: The prepared mTOR-NP showed the size of 257.3 nm and zeta potential of -32.5 ± 9.4 mV and drug release of 87.6% up to 48 hrs. The gel retardation results showed that mTOR siRNA integrity remained the same after conjugation with nanoparticles. Anticancer activity was confirmed by using MDA-MB231 cell-line and the antibody conjugated nanoparticles showed the significant anticancer activity. **Conclusion**: We are recommending that mTOR siRNA anchored PTX nanoparticles (mTOR NP) may have the ability to target the TNBC cells and improve the therapeutic action and subsidize the side effects of PTX.

Keywords: Triple negative breast cancer, PLGA-PTX nanoparticles, mTOR-siRNA, particle size distribution.

1.0 INTRODUCTION

Over the past few decades, with consistent developments in early diagnosis, the advancement of personalized treatment, strengthened chemotherapy, and there is a significant improvement in the survival rate of breast cancer patients. Nevertheless, breast cancer is still the main cause of cancer mortality among women worldwide. Basal-like breast cancer accounts for almost 15-20 % of breast cancers and has received much attention due to limited relapse-free and poor survival rates [1]. Several studies have shown that basal-like breast cancer type shared similar overlapping features with the triple-negative breast cancer (TNBC) that is identified by absence of ER, PR, and HER2 receptor expression. It is characterized by early relapse, lack of responsiveness to treatment, vigorous tumor formation, low mortality rate and distant recurrence [2]. At present, the cytotoxicity of chemotherapy and radiotherapy are permitted for early or advanced treatment for TNBC patients. Thus, this situation highlights the need for a novel discovery of molecular markers that specifically target the carcinogenesis and development of TNBC cells. It is indeed an urgent clinical need to enhance the diagnosis and treatment for TNBC patients [3]. Present tumour chemotherapy facing huge problems with lack of specificity of drug on tumour cell, leading to a limited therapeutic index of most anti-tumour drugs. In order to finding an effective therapeutic effect involves a high concentration of anti-tumour drugs around the cancer cells, which increases the chronic toxicity [4]. In order, to minimize the toxicity of the chemotherapy drug at its minimum dosage, unique nanoparticle delivery systems, such as nanoparticle, liposome, and polymeric micelle, may provide a promising treatment strategy due to its targeted delivery capabilities.

Poly (D-L-lactide-co-glycolide acid) (PLGA) polymer has been commonly used as an effective carrier for different drugs molecules, such as nucleotides and small compound, due to its sustained release capability, low toxicity, and biodegradability [5]. To date, many PLGA-based formulations have been approved for human use by the Food and Drug Administration. As a result, PLGA nanoparticles for the delivery of small interfering RNA (siRNA) have recently attracted attention as a promising delivery mechanism to the widely used polycation delivery methods which are non-biodegradable and/or unavoidably toxic [6]. The PLGA nanomaterial has gained a great attention as it meets the conditions necessary for optimal delivery of siRNA. It is effective for cellular uptake and tumour targeting, secondly the siRNA can be entrapped in the PLGA matrix, which provides physical protection against RNase activity as well as provide desirable colloidal stability. Basically, PLGA nanoparticles (NPs) have great controllable and modifiable degradation profile [7].

Recently, siRNA application provided us new types of drugs that are safe to use [8]. The siRNA relatively has high selectivity for strong inhibition expression of the gene in the cytoplasm. The main drawbacks of the therapeutic use of the siRNA are fast degradation of siRNA in the cellular cytoplasm and it will be easily excreted from the kidney [9]. In addition, siRNA molecules have poor tissue specificity and cellular uptake. Therefore, an ideal vector for the delivery of siRNA is required to increase their cellular uptake and prevent their excretion from the kidney. Paclitaxel (PTX), a mitotic inhibitor that is used in cancer chemotherapy, has proven its effectiveness against several forms of cancer, including advanced ovarian, lung and breast cancer. The anticancer role of the PTX includes the development of dysfunctional microtubules, the binding of microtubules, and causing cell death [10].

MTOR is a member of the PI3-kinase-related protein kinase (PIKK) family that acts as a central processor for the regulation of various cellular functions such as cell growth, proliferation, and survival [11]. Present study aims to synthesize PLGA NPs as carrier of paclitaxel and siRNA. Moreover, the mTOR signalling pathway has been shown to be crucially involved in the initiation, development, autoimmunity, metabolic disorders, resistance of cancer, cardiovascular disease, and ageing. Hence, the mTOR targeting pathway may be useful as an effective approach for the treatment of breast cancer.

2.0 MATERIALS AND METHODS

2.1 Preparation of siRNA anchored PTX loaded PLGA NPs

siRNA anchored PTX loaded PLGA NPs were prepared by a slight modifications of the double emulsion followed by solvent evaporation method [12] . About 50gm of PLGA was dissolved in 1 mL of dichloromethane (DCM). Separately dissolved 400mg of Bovine serum albumin in 100 µL of tris-EDTA (pH 9) and added 100 µL of siRNA with overtaxing. The siRNA mixture was added into PLGA organic solution and sonicated for one minute by keeping in ice bath, the sonicated mixture was slowly transfer into 3 mL of PVA [polyvinyl alcohol (2%)] and extended the sonication another 60 sec. the mixture was subjected to magnetic stirrer for 8 h to evaporate the organic solvent. The solution was subjected to centrifugation at 4°C (18000×g) for 10min and discarded the supernatant liquid. Collected the nanoparticle was precipitated and rehydrated with distilled water and the solution was freeze dried to get nanoparticle dry powder.

2.2 Encapsulation efficiency

Entrapment of efficiency (EE) and loading efficiency (LE) of siRNA entrapped into nanoparticles were acquired from the determination of free concentration of siRNA in the supernatant which recovered from centrifugation 13,000 × g for 30 mins at 4°C. The amount of siRNA entrapped within the PLGA NPs was measured by the difference between total amount of siRNA used and the amount present in the aqueous phase of supernatant. The absorbance measured at 260nm by using Nanodrop Spectrophotometer [13]. The supernatant was retrieved from the unloaded nanoparticles (without siRNA) have been used as a blank. The samples were analysed three times and the encapsulation efficiency (%) and loading efficiency (%) was calculated by using the following formula (F1) and (F2) :

$$\text{Entrapment efficiency (\%)} = \frac{\text{siRNA amount in loading buffer} - \text{siRNA amount in supernatant}}{\text{siRNA amount in loading buffer}} \times 100\text{-----F1}$$

$$\text{Loading efficiency (\%)} = \frac{\text{Total amount of entrapped siRNA}}{\text{Total amount of NPs}} \times 100\text{---------F2}$$

2.3 Transmission Electron Microscopy (TEM) analysis

TEM was used to detect the morphology of nanoparticles. The electron beam was transmitted through an ultra-thin layer, reacting with the material as it travels through it. An image formed from the interaction of the electrons, when transmitted through the sample was magnified, and subsequently focused on the imaging device. A sample drop was mounted on a carbon-coated grid, made of copper, leaving a thin film on the grid. Once the film was fully dried on the board, the film was coated with 1 % phosphotungtic acid (PTA). A drop of the staining solution was applied to the film and the excess solution was removed with a filter paper. The grid was then allowed to dry completely before scanning under the transmission electron microscope.

2.4 Measurement of the nanoparticle size, poly dispersity index (PDI) and zeta potential

The size of nanoparticle was measured by the photon correlation spectroscopy method on the Zetasizer. Freeze dried nanoparticles (10 mg) were dissolved in 5 mL of distilled water and analysed at a temperature of 25°C using the Malvern Zetasizer NanoZS (United Kingdom) instrument. The diameter was determined based on the autocorrelation function of the strength of light emitted from nanoparticles. The polydispersity index (PDI) is an indicator of

dispersion homogeneity. The PDI was calculated for dispersion homogeneity ranging from 0 to 1. The value close to 0 indicated a homogeneous dispersion and value greater than 0.7 indicate high heterogeneity [14–16]. The surface charges of the nanoparticles were evaluated by measuring the zeta potential. The zeta potential is a major indicator of the stability of the colloidal dispersion. The zeta potential indicates the degree of electrostatic repulsion between nearby, similarly charged particles in the dispersion. Nanoparticles with high zeta potential confers stability. Samples were diluted with distilled water and measured using the Malvern Zetasizer NanoZS instrument at a temperature of 25ºC. The instrument operated with a HeNe laser operating at 632.8 nm.

2.5. Fourier Transform Infra-Red (FTIR)

The FTIR analysis was done to characterize the the compatibility between drug and polymer by using Shimadzu FTIR8400S, Japan instrument. The FTIR spectra of samples were recorded using the potassium bromide (KBr) disc technique [17]. Samples equivalent to 2mg of free PTX, PLGA and the PTX NPs were mixed with KBr pellet (100mg) and compressed to make a pellet. The baseline was corrected, and the samples were scanned in the IR range from 4000 to 400 cm-1.

2.6 Differential Scanning Calorimetry (DSC)

The DSC gives an understanding of melting behaviour, polymorphism, purity, glass transition, crystallization, compatibility, and chemical reactions of drugs such as stability and decomposition kinetics. In this study, PLGA, PTX and PTX NPs were subjected to temperature variations using differential scanning calorimetry (Shimadzu DSC-60). Samples were heated in a range of between 25°C-300°C using an aluminium pan and heat increased by of 10°C per min under the nitrogen gas with a flow rate of 40 mL/min. The DSC spectra were interpreted to understand the compatibility of the drug with the polymer in the formulations.

2.7 X-ray Diffraction (XRD) analysis

XRD analysis provides a great amount of knowledge on the crystalline composition of the materials used. The PLGA, PTX and PTX NPs were tested using the Bruker D8 Advance diffractometer system (Bruker AXS, USA). It operated at a wavelength of (λ Cu Kα 11,54059Å), 43 kV and 25 mA in Bragg-Brentano geometry using the LynxEye detector. The scanning was conducted from 10° to 80° at a scanning rate of 10/min.F.

2.8 MTT Assay

MDA-MB-231 cell-lines have been obtained from the American Type Culture Collection (ATCC) and incubated at 37°C for cell growth. The base medium for this cell-line was purchased from Addexbio Leibovitz L-15 Medium (USA). Cell growth was achieved by adding 0.01 mg/mL of penicillin/streptomycin and 10 % fetal bovine serum (FBS) to the final concentration [11]. The MDA-MB-231 cell-line was used for a cytotoxicity study by 3-(4,5 -dimethylthiazol-2-yl)-2,5-diphenyltetrazolium bromide (MTT) tetrazolium reduction test. The cell metabolic activity of the three formulations PTX and PTX NPs and mTOR NPs were compared using the MTT assay. MDA-MB-468 cells (2×10^4 plated cells / well) were seeded in 96 well plates and incubated for 24 hrs for partial monolayer was formed. The cells were incubated with different concentration (0.2, 2, 20, 25 μg/mL) to determine the IC_{50} value of PTX. After 24 hrs of incubation time, the culture medium was extracted and 20μL MTT reagent (5mg/mL in PBS) was added to each well and incubated for 4 hrs to produce formazan. The medium was discarded and 100μL of dimethyl sulfoxide (DMSO) was added to dissolve the pink colour formazan and further incubated at 37°C for 30 mins. Absorption of the plates were read at 640nm using a microplate reader (Tecan Deutschland GmbH, Crailsheim, Germany). The samples were analysed three times and the cell viability (%) was calculated by using the following formula (F3) and the IC_{50} value of PTX was calculated using Microsoft Excel 2011. Similarly, an equivalent amount of IC_{50} concentration of PTX loaded in the NP. This assay was followed for 24 hrs and 48 hrs of incubation and the results were compared with blank and control.

$$\text{Cell viability (\%)} = \frac{\text{OD treated well}}{\text{OD control well}} \times 100 \text{----------F3}$$

2.9 Cell viability assay

The MDA-MB 231 and MCF-12A (control cell-line) cells were seeded in a 6-well plate of 2×10^5 mL of DMEM and Leibovits media that contained 10% v/v of FBS and 1% w/v penicillin-streptomycin antibiotic mixture. After 24 hrs of treatment with or without 5% CO_2 at 37°C, cells were cultured until they reached 70 to 80% confluence. The medium was then substituted with 1 mL of serum-free medium. The final concentration 100 nmol/L of mTOR NPs, PTX NPs and PLGA NPs were used in this experiment. The medium was changed after 6h of incubation and replaced with the DMEM and Leibovits medium containing 2% serum and then was incubated at 37°C for an additional 24 hrs and 48 hrs. The cells were collected to determine the cell viability by using Trypan blue exclusion assay.

2.10 *In-vitro* release

The drug release behavior of the nanoparticles was investigated using the following dialysis method where, 30mg nanoparticles (pure PTX, PTX NP and mTOR NP) were added separately into 100 mL of phosphate buffer solution (pH 7.4) and maintained at 37°C with stirring speed at 100rpm. Each time, 4 mL of dialysate was collected from the released medium and replaced with fresh PBS. The drug release studies of all batches were performed in triplicate to confirm the reproducibility of the analysis. The absorbance was read with a UV-visible spectrophotometer at a wavelength of 228nm.

3.0 RESULTS AND DISCUSSION

3.1 Physiochemical parameter of siRNA loaded PLGA nanoparticle-

A modified double emulsion solvent diffusion method was used to prepare the formulation from the PLGA polymer which contains free carboxylic end groups. The TEM methods were used to determine the morphology of NP as shown in figure 1 for the mTOR NP (Figure 1a) and PTX NP (Figure 1b). The TEM images displayed a spherical shape with a smooth surface and without aggregation. The developed nanoparticles had a mean diameter of 200–360 nm with the polydispersity index of 0.243 (Figure 2 a). The mean value of the zeta potential of NPs was −6.86 mV (Figure 2 b). Zeta potential of NPs was negative due the surface of NPs having certain free carboxylic end groups of the polymer [18]. This nanoformulation is suitable to obtain an effective intracellular uptake of nanoparticles. Circulating nanoparticles must break through leaky capillaries to reach and accumulate in tumour tissues. As a result, in this study, we concentrated on producing NPs with a size range of 300nm. The NP diameter for all three formulations remained between 190 nm and 300nm, which is the appropriate size range for efficient cellular uptake.

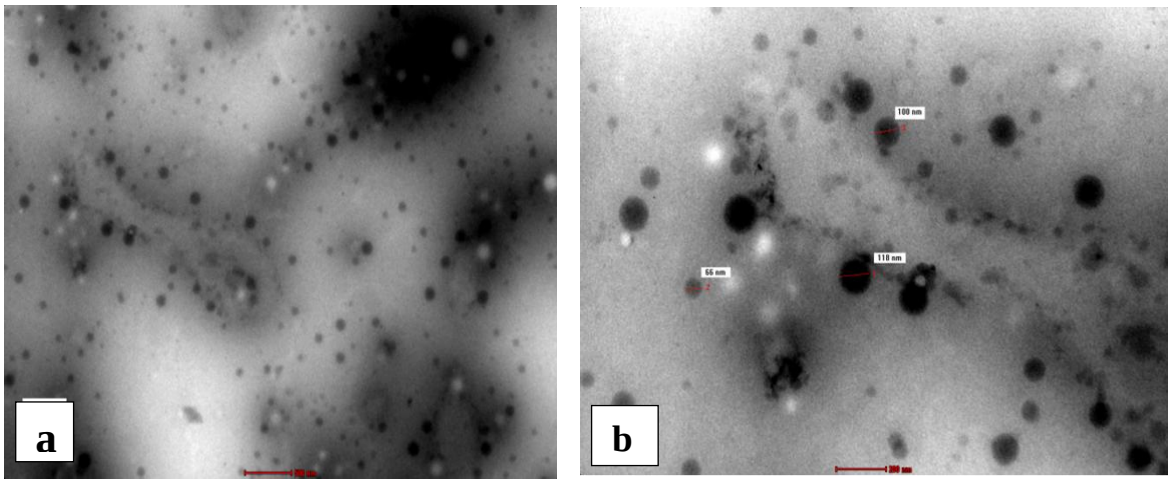

Figure 1: Transition Electron Microscope (TEM) images of (a) mTOR NP and (b) PTX NP.

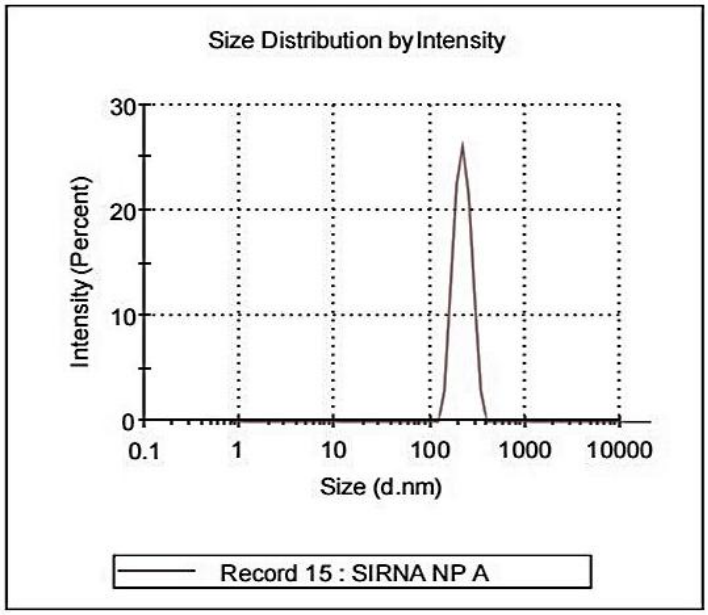

Figure 2 (a): Size distribution of optimized formulation.

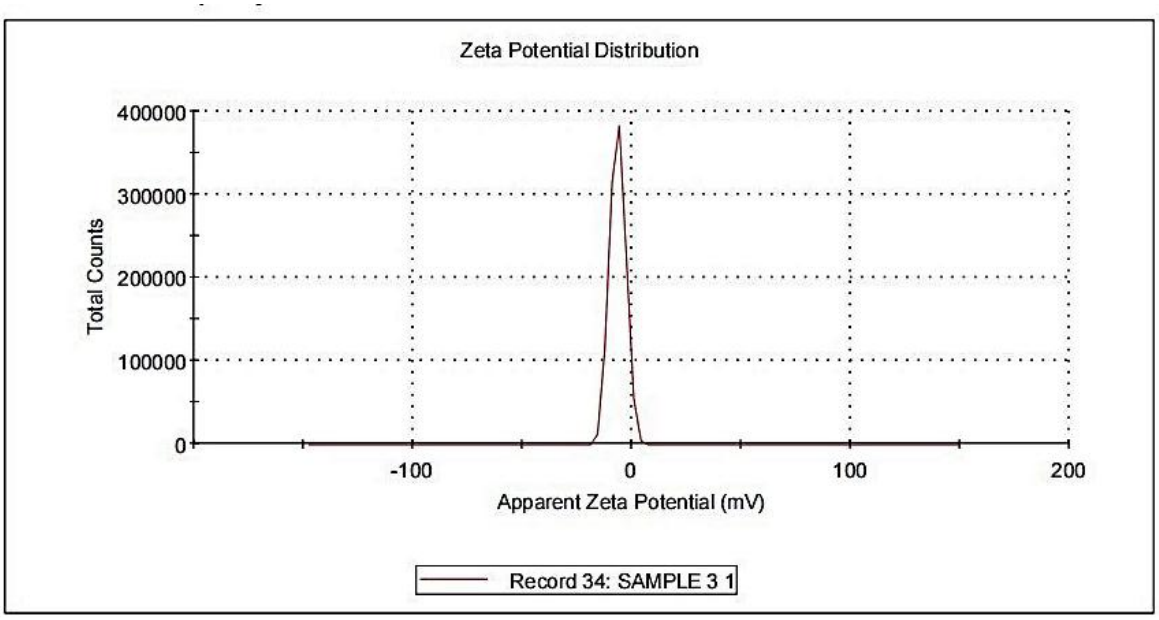

Figure 2 (b): Zeta potential distribution of optimized formulation.

3.2 FTIR

FTIR spectroscopy was done to confirm the effective conjugation of PTX with PTX-NP. PLGA, pure PTX and PTX NP were subjected to FTIR spectrophotometer and are shown in figure 3. The PTX NP peaks can be observed at ~1750, 1620, 1600 and 750 cm^{-1} due to the C-H stretching of methylene groups, N-H stretching vibration C-O stretching vibrations and

C=O stretching vibrations respectively [19]. In the FTIR spectra of PTX spectrum, a peak of ~1,360 cm-^{1} was observed because of the stretching of the O-H groups. The aliphatic C-H spectrum was observed at ~750 cm-^{1}. Further, the stretching frequency of the aromatic C-H bonds, aromatic ring (C=C) and C=O amide stretching of PTX were observed. The existence of PTX peaks in the FTIR spectrum of PTX NPs confirmed the conjugation of PTX to the surface of PTX NPs. So, after the esterification, the C=O stretching vibration associated with the PLGA NPs carboxylic acid end group was transitioned to the upper frequency. This frequency shift upon the esterification confirmed the conjugation of PTX on the surface of PTX NPs. Peaks for drugs were appeared in formulations due to which the drug was entirely trapped in the polymeric amorphous or polymeric surface [20]. The results of the FT-IR studies revealed no evidence of chemical or physical interaction between drugs and excipients. PTX trapped inside the PLGA polymer matrix without chemical alterations and interactions.

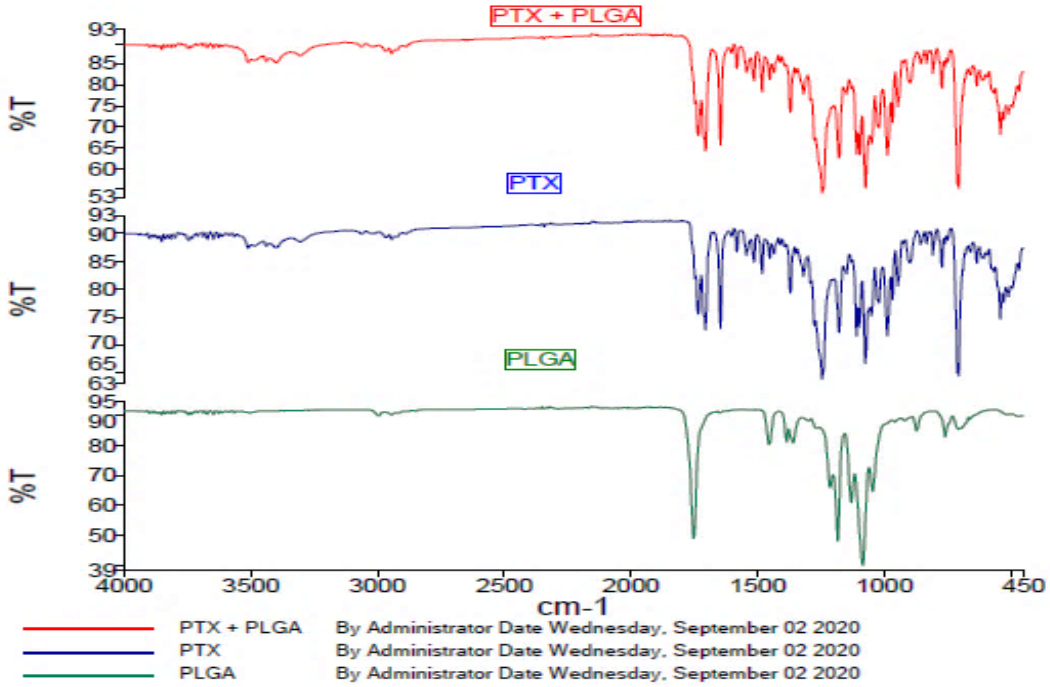

Figure 3: FTIR spectra of pure PLGA, pure PTX and PTX NP.

3.3 DSC

DSC provides supporting confirmation for the preparation of the PTX NPs. Figure 4 shows the thermograms of pure PTX, PTX-NPs. Thermograms indicate melting points of PTX at 225 °C which demonstrates that it is crystalline in nature (Figure 4a). The DSC thermogram for PTX showed a single endothermic peak at 225 °C but there was no peak visible near the melting point of PTX NPs thermogram, which confirmed the formation of conjugate and the

absence of any unconjugated PTX in the product. DSC samples were heated from 0-230°C to avoid chemical changes in PTX. As shown in Figure 4b, the melting points of PTX shifted to a higher temperature after coating on the surface of the PLGA, that confirming the coating of PLGA with PTX. The DSC thermograms generated their respective endothermic values demonstrated that the drug and the implant preparation method had very little effect on the polymer's thermal properties. However, the drug peak did not appear which may be due to the conversion of PTX from crystalline to amorphous or dissolved during the heating process involved in the preparation of the implant. Another phenomenon can be expected as elevated temperature and a slow cooling rate causes the chains to be mobile and can result in a semi crystalline or amorphous nature or drug in the polymeric amorphous surface to realign.

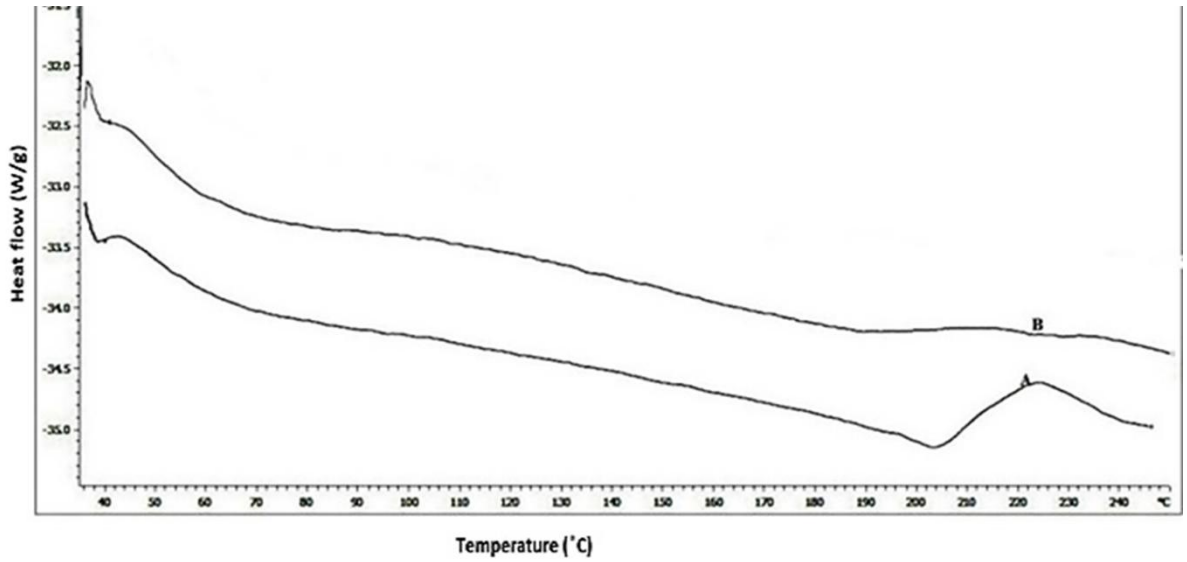

Figure 4: DSC thermograms shows (A) Free PTX and (B) PTX-NP

3.4 XRD

It is necessary to interpret crystalline forms as an arrangement of molecular chains leading to an ordered structure. Polymers are generally crystalline, semi-crystalline or amorphous. There are crystalline regions in crystalline polymers such as PLGA. Parameters that affect a polymer's crystallinity are those that provide polymeric molecular chains to reorganize into a more ordered state of energy, thereby reducing the energy state. The high temperature and a slow cooling rate make it possible for the chains to be mobile and realign themselves in a solid structure that is more orderly. Because of the heat involved in the melting process, the crystallinity of the PLGA polymer can also be altered, as the degree of crystallinity also relies on the rate of cooling during solidification from the melting. Illustration of the XRD spectra of pure PTX, polymer, physical mixture and developed implants is provided figure 5. Sharp

peaks were obtained at 13.5, 16.5 (2θ) of pure PTX. PTX NP shows the absence of drug peak in developed implants which further justified the presence of drug in the form of amorphous or dissolution state.

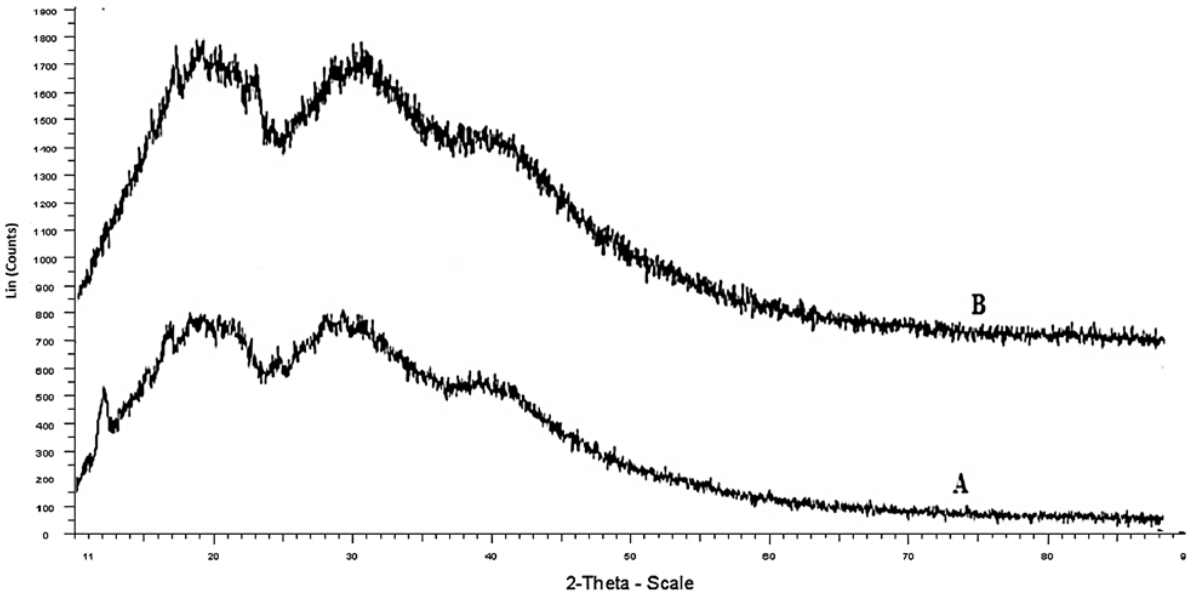

Figure 5: X-ray diffraction for (A) Free PTX and (B) PTX NP

3.5 *In-vitro* drug release analysis

The *in-vitro* release studies have been performed to establish the comparative release pattern for pure PTX, PTX-NP and mTOR-NP previously reported by [20]. The phosphate buffer (pH 7.4) was used for the *in-vitro* release studies (Figure 6). The release medium was chosen because PTX is highly lipophilic and ionization behaviour is Zwitterionic and does not have ionizable groups with pKa values in the physiological pH range. This analysis was conducted on lyophilized nanoparticles. There was a pronounced time prolongation of drug release from the nanoparticles. About 85% of free drug (PTX) released was observed with 15 hrs. The result of the initial burst of mTOR NP is important and the cumulative quantity of PTX released increased to 43.9% in 12 hrs to 62% at 48 hrs. The mTOR NP formulation showed sustained release of drug throughout the experiments. Moreover, it showed an initial burst release of PTX during the first 4 hrs of incubation due to the diffusion of the dissolved drug accumulated within the pores of the nanoparticles may be the source of the initial burst release [21]. The high surface-to-volume ratio of the geometry of the nanoparticle is indeed responsible for the release of eruptions [22]. The release pattern of the mTOR NP is much slower than PTX. It is noticeable that the non-encapsulated drug (PTX) was more quickly

released into medium than the encapsulated mTOR NP). It also observed that the low PTX amount exhibited a release in a more sustained manner [23].

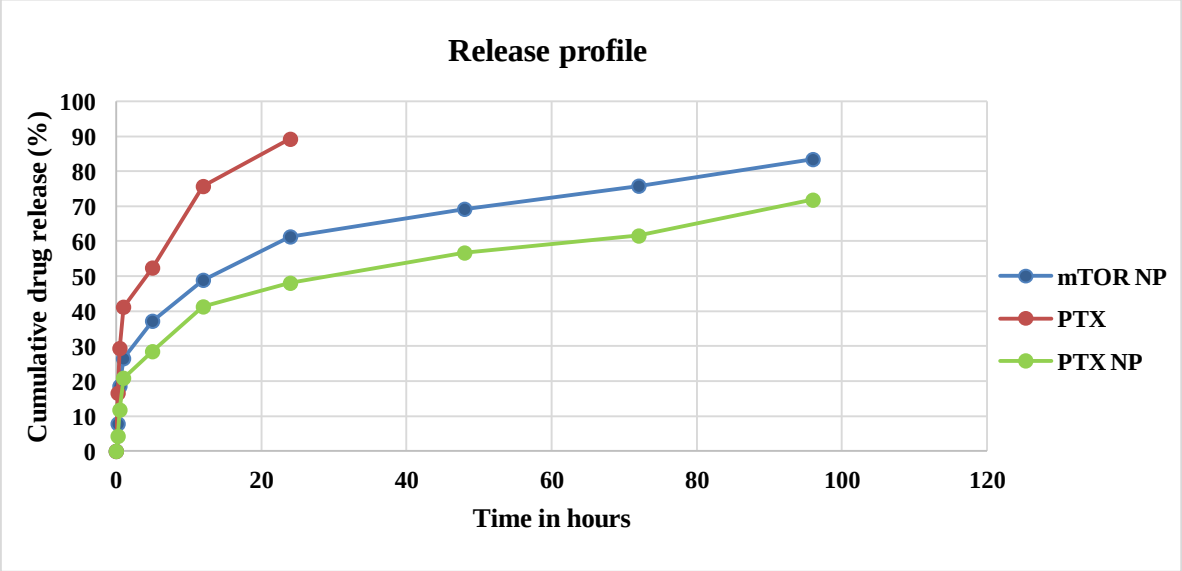

Figure 6: Release profile of pure PTX, PTX NP and mTOR NP.

3.6 Entrapment efficiency

One of the most important dependent variables is the encapsulation efficiency of a drug in a NPs is the entrapment efficient. The purpose of this experiment was to optimize the encapsulation efficiency of the NPs. However, influence factors of entrapment efficiency on this technique are very complicated, such as copolymer concentration in organic solution, volume of inner aqueous phase, volume of outer aqueous phase, protein concentration in inner aqueous phase, the first homogenized speed, time and PVA concentration. Both the volume ratio and the PLGA concentration are strongly associated with the capacity of encapsulation, indicating that an increase in these parameters causes the siRNA's encapsulation efficiency to increase.

For all the formulation, initially there was burst release of PTX for both formulations. The fast release could be obtained from the PTX that absorbed onto the wall of NPs that would be immediately released during the initial phase. Later, the PTX release profile maintained a sustained manner. The sustained release may be due to the diffusion of PTX from the wall of polymer as well as the degradation of the polymer. The faster and higher PTX release was observed on free PTX formulation which was about 64.8% than PTX-NP (51.2%) and mTOR-NP (56.4%) at 24 hrs (Table 1). The different range of the entrapment efficiency between the NPs could be due to the presence of PLGA chain. The presence of protein

molecules on the surface of NPs (mTOR-NP) could cause the immediate release during the initial stage. After 48h, the entrapment efficiency of mTOR-NP achieved 87.6%, PTX-NP (78.3%), and free PTX (70.3%). These results showed that mTOR-NP could be effective carrier for better drug delivery formulation and would be beneficial for prolonged drug release [24].

Table 1: Entrapment efficiency

Nanoformulation	**Size (nm)**	**Zeta potential (mV)**	**Entrapment efficiency (%)**
PTX	198.3	-15.8±10.5	64.8
PTX NP	239.5	-29.6±11.2	51.2
mTOR-NP	257.3	-32.5±9.4	56.4

3.7 Cytotoxicity Analysis

The cytotoxicity of PTX NP and mTOR-NP were evaluated by assessing the cell viability by MTT assay using MDA MB 231 cell-line. The dose-dependent cytotoxicity was observed at concentrations of 0.2–25 µg/mL. This concentration was chosen because it matches to the plasma levels of drug achievable in human [25]. The viability of cell was significantly decreased at higher concentrations. The cytotoxicity of PTX NP and mTOR were characterized by MTT assay method using MDA-MB-231 breast cancer cells. Initially, the IC_{50} value of PTX was determined by the various concentrations of PTX and it was found to be 2.27 ± 0.2µg/mL (Figure 7).

The PLGA are commonly known as low-level cytotoxicity with great biocompatibility, biodegradability is actively used human beings for resorbable bone, sutures, and contraceptive implants [6]. Figure 8 showed that a greater reduction in cell viability when MDA MB 231 cells were incubated with 20µg/mL of PTX NP and mTOR NP. There was no noticeable difference between PTX NP and mTOR NP. This confirms the relative stability of PTX compared to mTOR-NP. Therefore, mTOR NP is a potent therapeutic carrier with no major cytotoxic consequences. However, at the lower concentration (0.025 and 0.25µg/mL) of PTX NP shows 17% of reduction in cell viability at initial stage but over longer incubation times no significant changes in the cytotoxicity among the two concentrations. A drastic reduction in cell viability was observed when the cells were incubated to 2.5µg/mL. Nevertheless, for the longest incubation time (72 hrs) a marked cytotoxic effect could be

observed for both 2.5 and 25µg/mL. mTOR-NP were showed the similar levels of toxicity to those for 25µg/mL PTX NP. For mTOR-NP, after 1 hr of incubation, no cytotoxicity effect was observed from any of the concentrations but increasing in the incubation times resulted increasing the cytotoxicity of mTOR-NP.

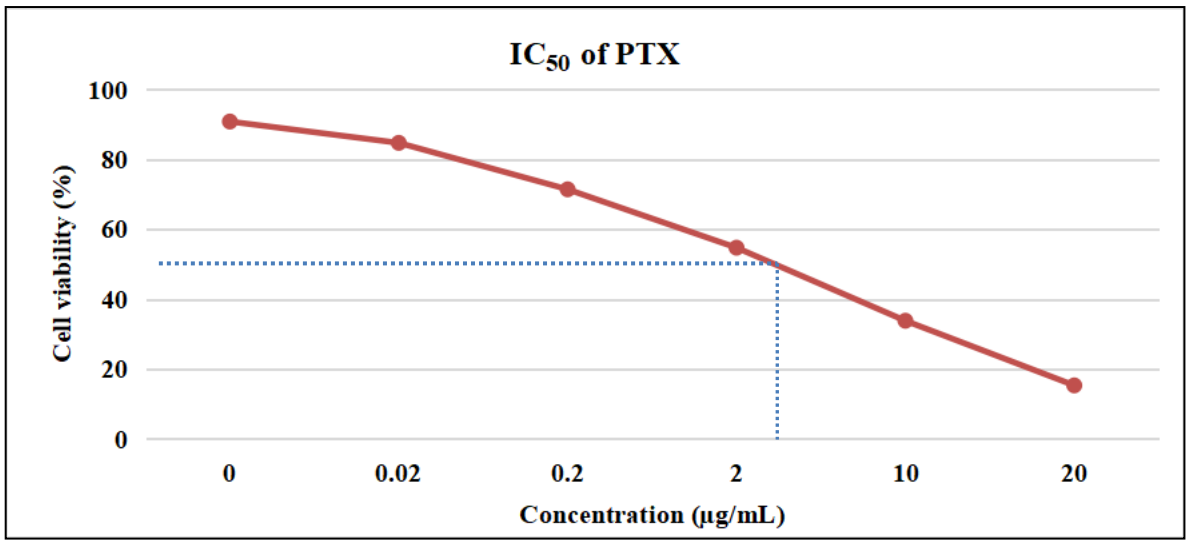

Figure 7: Cell viability studies of different concentration of PTX incubated in MDA-MB-231 breast cancer cell-line. "The cancer cells were incubated with 0.02, 0.2, 2, 20 µg/mL concentrations of PTX.

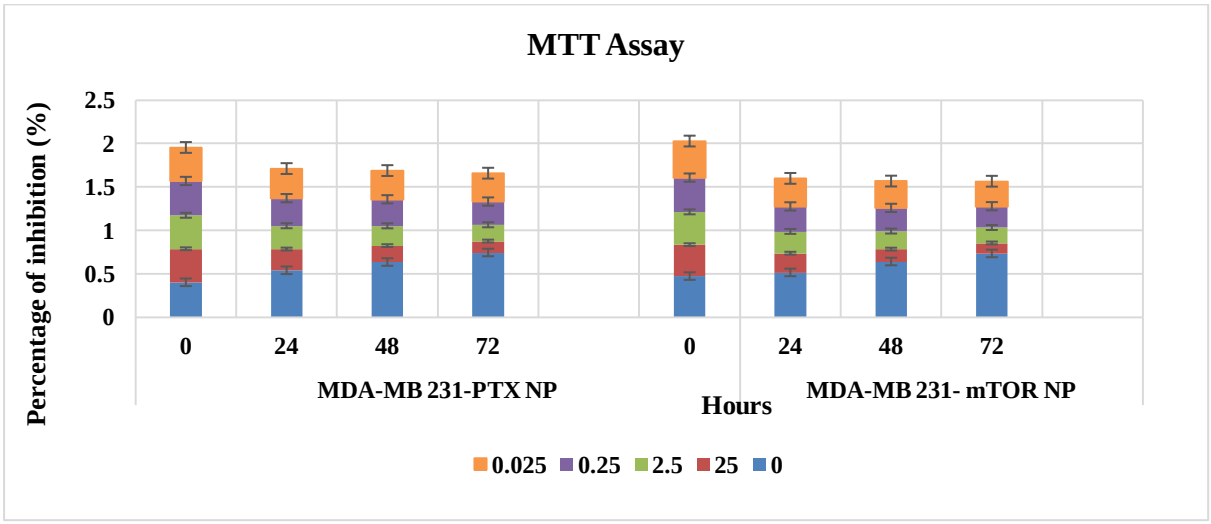

Figure 8: Percentage of cell inhibition of PTX NP and mTOR NP at different concentration (0.02, 0.25, 2.5, 25 µg/mL)

4.0 CONCLUSION

The study achieved its objective for developing objective was achieved by developing a polymeric nanoparticles drug delivery system for PTX using PLGA and mTOR siRNA with controlled release. The anti-tumour activity was demonstrated for the first time against MDA MB 231 cell-lines. The methodology used in this study supported the immediate and repeatable fabrication of nanoparticles with homogeneous and spherical morphology. The siRNA nanoparticles demonstrated high drug encapsulation and loading efficiency. The in-vitro release study revealed that siRNA nanoparticles had a slow and sustained-release phenomenon over a long period of time. The siRNA nanoparticle siRNA reduces the cancer cell migration and congenic potential. As a result, the formulation developed in this study can be regarded as a promising and effective anticancer drug delivery system for long-term treatment of triple negative breast cancer (TNBC). However, more research is needed to determine the extent of anticancer efficacy of the current siRNA nanoparticle in an in-vivo TNBC cancer model system.

Ethics approval and consent to participate

Not applicable.

Human and animal rights

No animals/humans were used for studies that are the basis of this research.

Consent for publication

Not applicable.

Funding

This research has been funded by the Fundamental Research Grant Scheme (FRGS) under a grant number of FRGS/1/2017/SKK08/AIMST/02/3 from the Ministry of Education Malaysia.

Availability of data and materials

Not applicable.

Conflict of interest

None.

Acknowledgements

The authors are grateful for the support and facilities provided by AIMST University and the Oncological and Radiological Sciences Cluster, Advanced Medical and Dental Institute, University of Science and Technology of Malaysia (USM).

REFERENCES

[1] Trop I, LeBlanc SM, David J, Lalonde L, Tran-Thanh D, Labelle M, et al. Molecular Classification of Infiltrating Breast Cancer: Toward Personalized Therapy. https://doi.org/101148/rg345130049 [Internet]. 2014 Sep 10 [cited 2021 Oct 5];34(5):1178–95.

[2] Krutovskikh VA, Herceg Z. Oncogenic microRNAs (OncomiRs) as a new class of cancer biomarkers. *BioEssays* [Internet]. 2010 Oct 1 [cited 2021 Oct 5];32(10):894–904.

[3] Andreopoulou E, Kelly CM, McDaid HM. Therapeutic Advances and New Directions for Triple-Negative Breast Cancer. *Breast Care* [Internet]. 2017 Mar 1 [cited 2021 Oct 5];12(1):20–7.

[4] Kassam F, Enright K, Dent R, Dranitsaris G, Myers J, Flynn C, et al. Survival Outcomes for Patients with Metastatic Triple-Negative Breast Cancer: Implications for Clinical Practice and Trial Design. *Clin Breast Cancer* [Internet]. 2009 [cited 2021 Oct 5];9:29–33.

[5] Kwak SY, Lee S, Han HD, Chang S, Kim K, Ahn HJ. PLGA Nanoparticles Codelivering siRNAs against Programmed Cell Death Protein-1 and Its Ligand Gene for Suppression of Colon Tumor Growth. *Mol Pharm* [Internet]. 2019 Dec 2 [cited 2021 Oct 5];16(12):4940–53.

[6] Devulapally R, Sekar NM, Sekar T V., Foygel K, Massoud TF, Willmann JK, et al. Polymer Nanoparticles Mediated Codelivery of AntimiR-10b and AntimiR-21 for Achieving Triple Negative Breast Cancer Therapy. *ACS Nano* [Internet]. 2015 Mar 24 [cited 2021 Oct 5];9(3):2290–302.

[7] Hines DJ, Kaplan DL. Poly (lactic-co-glycolic acid) controlled release systems: experimental and modeling insights. *Crit Rev Ther Drug Carrier Syst* [Internet]. 2013 [cited 2021 Oct 5];30(3):257.

[8] Hu B, Zhong L, Weng Y, Peng L, Huang Y, Zhao Y, et al. Therapeutic siRNA: state of the art. *Signal Transduct Target Ther* 2020 51 [Internet]. 2020 Jun 19 [cited 2021 Oct

5];5(1):1–25.

[9] Cun D, Foged C, Yang, M, Frøkjaer S, Nielsen H. Preparation and characterization of poly(DL-lactide-co-glycolide) nanoparticles for siRNA delivery. *Int J Pharm* [Internet]. 2010 May [cited 2021 Oct 5];390(1):70–5.

[10] Gornstein EL, Schwarz TL. Neurotoxic mechanisms of paclitaxel are local to the distal axon and independent of transport defects. *Exp Neurol* [Internet]. 2017 Feb 1 [cited 2021 Oct 5];288:153.

[11] Wang F, Yuan J, Zhang Q, Yang S, Jiang S, Huang C. PTX-loaded three-layer PLGA/CS/ALG nanoparticle based on layer-by-layer method for cancer therapy. https://doi.org/101080/09205063201814759 41 [Internet]. 2018 Sep 2 [cited 2021 Oct 5];29(13):1566–78.

[12] Hassan B, Akcakanat A, Holder AM, Meric-Bernstam F. Targeting the PI3-kinase/Akt/mTOR Signaling Pathway. *Surg Oncol Clin N Am* [Internet]. 2013 Oct [cited 2021 Oct 5];22(4):641–64.

[13] Patil Y, Panyam J. Polymeric nanoparticles for siRNA delivery and gene silencing. *Int J Pharm*. 2009 Feb 9;367(1–2):195–203.

[14] Afrooz H, Ahmadi F, Fallahzadeh F, Mousavi-Fard SH, Alipour S. Design and characterization of paclitaxel-verapamil co-encapsulated PLGA nanoparticles: Potential system for overcoming P-glycoprotein mediated MDR. *J Drug Deliv Sci Technol*. 2017 Oct 1;41:174–81.

[15] Alibolandi M, Ramezani M, Abnous K, Sadeghi F, Atyabi F, Asouri M, et al. In vitro and in vivo evaluation of therapy targeting epithelial-cell adhesion-molecule aptamers for non-small cell lung cancer. *J Control Release*. 2015 Jul 10;209:88–100.

[16] Kumar R, Pahal V, Singh J. Prevalence of Genotype D and Precore/Core Promoter Mutations in Hepatitis B Virus-infected Population of North India. *J Clin Exp Hepatol*. 2011 Sep 1;1(2):73–6.

[17] Sahil A, Swati G, D P, RS M. Gemcitabine-loaded PLGA-PEG immunonanoparticles for targeted chemotherapy of pancreatic cancer. *Cancer Nanotechnol* [Internet]. 2013 Dec [cited 2021 Oct 5];4(6):145–57.

[18] Zhao Z, Li Y, Zhang Y. Preparation and characterization of Paclitaxel loaded SF/PLLA-PEG-PLLA nanoparticles via solution-enhanced dispersion by supercritical CO2. *J Nanomater*. 2015;2015.

[19] Lu B, Lv X, Le Y. Chitosan-Modified PLGA Nanoparticles for Control-Released Drug Delivery. *Polymers* (Basel) [Internet]. 2019 Feb 12 [cited 2021 Oct 7];11(2).

[20] Devi TSR, Gayathri S. FTIR and FT-RAMAN Spectral analysis of paclitaxel drugs. *Int J Pharm Sci Rev Res* [Internet]. [cited 2022 Jul 26];2(2).

[21] Xu S, Wang W, Li X, Liu J, Dong A, Deng L. Sustained release of PTX-incorporated nanoparticles synergized by burst release of DOX·HCl from thermosensitive modified PEG/PCL hydrogel to improve anti-tumor efficiency. *Eur J Pharm Sci.* 2014 Oct 1;62:267–73.

[22] Cui F, Li Y, Zhou S, Jia M, Yang X, Yu F, et al. A comparative in vitro evaluation of self-assembled PTX-PLA and PTX-MPEG-PLA nanoparticles. *Nanoscale Res Lett* 2013 81 [Internet]. 2013 Jun 27 [cited 2021 Oct 5];8(1):1–8.

[23] Jeevanandam J, Barhoum A, Chan YS, Dufresne A, Danquah MK. Review on nanoparticles and nanostructured materials: history, sources, toxicity and regulations. *Beilstein J Nanotechnol* [Internet]. 2018 Apr 3 [cited 2021 Oct 7];9(1):1050.

[24] Liu J, Zhang L, Yang Z, Zhao X. Controlled release of paclitaxel from a self-assembling peptide hydrogel formed in situ and antitumor study in vitro. *Int J Nanomedicine* [Internet]. 2011 [cited 2021 Oct 5];6:2143.

[25] S F, G K, E R. Current development of mTOR inhibitors as anticancer agents. *Nat Rev Drug Discov* [Internet]. 2006 Aug [cited 2021 Oct 5];5(8):671–88. A